Journal of
Ceramic Science
and Technology

J. Ceram. Sci. Tech., **05** [02] 77-82 (2014)
DOI: 10.4416/JCST2013-00033
available online at: http://www.ceramic-science.com

Influence of Temperature Dependence of Bulk Modulus on Crack Propagation Velocity

D. Pilipenko, Y. Natanzon*, H. Emmerich

Material and Process Simulation Group, University of Bayreuth
Universitätsstrasse 30, 95447 Bayreuth, Germany

received October 21, 2013; received in revised form December 19, 2013; accepted January 22, 2014

Abstract

Multiscale modeling of crack propagation in homogeneously heated aluminium oxide is presented. It is known that the crack propagation velocity depends on both the bulk modulus and surface energy of a material. The temperature dependence of surface energy is often ignored owing to the difficulty associated with obtaining a reliable measurement. Such dependence was calculated in atomic-scale calculations by means of Molecular Dynamics with MEAM potential. The dependence shows a linear decrease with an increase in temperature. The MD results are used as input for phase field simulations of fracture. It is shown that if only the temperature dependence of the bulk modulus is taken into account the crack velocity decreases by 30 %. However, only a 2 % decrease is observed when both the temperature dependence of surface energy and bulk modulus are considered.

Keywords: Fracture mechanics, fatigue and cracks, high-temperature ceramics, computational methods in continuum mechanics, multiscale modeling

I. Introduction

Owing to the resulting high thermal shock resistance, carbon is used in more than 40 % of all refractories worldwide to adjust their thermomechanical and chemical properties. For the development of 'cleaner' high-temperature ceramics and the consequential avoidance of carbon it is essential to understand how other materials can be tailored to reach comparable thermal shock resistance even when exposed to today's higher thermal shock stresses.

α Aluminium oxide (corundum) is one such promising refractory material with a melting temperature of 2000 K and fracture toughness of 2.30 MPa×m$^{1/2}$ [13]. While its elastic properties and critical tensile strain have been determined effectively [13], little is known about damage evolution in this material. Crack growth in alumina can be either hindered or promoted by the presence of various additives. For example, water is found to trigger subcritical crack growth with a rate of 10^{13} m/s [16], while iron additives increase its fracture toughness [25].

On atomic level, cracks are created by the breaking of bonds resulting from either an applied load or a chemical reaction. The resulting nano-cracks interact with each other and then propagate to the macroscale. Such processes cannot be described with mesocale methods as continuum mechanics breaks down on the nano-scale [18]. Thus damage evolution is a multiscale process which requires comprehensive understanding of crack propagation in alumina on both atomic scale and macroscale.

* Corresponding author: yuriy.natanzon@uni-bayreuth.de

The fundamental basis of today's understanding of the fracture phenomenon is traced back to Griffith [10], who realized that the growth of cracks is determined by a competition of a release of elastic energy and a simultaneous increase of the surface energy owing to the advancing crack. Since this time, the motion of a crack has been relatively well understood in the framework of continuum theories [6, 9]. The crack is treated as a front or interface separating broken and unbroken regions of the material and its propagation is governed by the balance of the elastic forces in the material and cohesive stresses near the crack [1, 2, 14].

On the other hand, both elastic and surface energies are dependent on both the crystal structure of the material and its chemical composition, and can be determined with either quantum mechanical methods such as Density Functional Theory (DFT) or classical Molecular Dynamics (MD) where empirical potentials mimic the covalent bonding. DFT [15] is based on the solution of Schrödinger-like equations for electrons and accurately describes the electronic structure of the material from first principles. However, this method is both computationally demanding and is only applicable at 0 K. In contrast, Molecular dynamics is based on the solution of Newton equations for atoms moving in external potential, where temperature can be easily introduced via external kinetic energy. This allows consideration of systems consisting of millions of atoms, which is important for crack propagation modeling. The accuracy of such calculations requires sophisticated fitting of the interatomic potential parameters to known material properties.

In this paper we report on the multi-scale modeling of crack propagation in homogeneously heated alumina. For this purpose Molecular Dynamics with Modified Embedded Atom Method (MEAM) [7, 20, 28] interatomic potential was chosen, as this potential is partly derived from the DFT method. The potential parameters were fit to correctly reproduce the lattice constants and elastic moduli of alumina. Then, the temperature dependence of the surface energy was calculated and the results obtained were used as input for phase field simulations to study crack growth under mode I loading with a temperature gradient created along the crack propagation direction.

II. Molecular Dynamics Calculations of Surface Energy

Surface energy is defined as half the energy needed to separate a material into two pieces, this quantity defines the critical strain energy needed to facilitate crack growth. Calculating the surface energy with atomistic simulations is particularly handy when experimental data is not available. Since atoms inside the crystal are more tightly bound to each other than atoms at the surface, a system with a surface will have lower energy than periodic bulk crystal. The difference between two energies will give us the surface energy as defined in [12, 19]:

$$\gamma = \frac{E_{total}^{fracture} - N_{atoms} E_{total}^{bulk}}{2S_A} \quad (1)$$

where $E_{total}^{fracture}$ is the calculated total energy of fractured material with two surfaces separated (as shown in Fig. 1), S_A is the surface area, N_{atoms} is the number of atoms in the fractured material and E_{total}^{bulk} is per atom bulk energy of undistorted alumina crystal (where two surfaces are together).

Total energies in these two calculations are obtained as a sum of kinetic energy and pair interaction energy which is determined by interatomic potential:

$$E_{total} = E_{pair} + E_{kinetic} \quad (2)$$

For the pair interaction energy the Modified Embedded Atom Method (MEAM) was used, in which it is calculated with the following equation [3, 7]:

$$E_{pair} = \sum_i \left\{ F_i(\overline{\rho_i}) + \frac{1}{2} \sum_{i \neq j} V_{ij}(r_{ij}) \right\} \quad (3)$$

where $V_{ij}(r_{ij})$ is a pair interaction potential between atoms i and j, F_i is the embedding function, which depends on the background electron density $\overline{\rho_i}$ [28]:

$$F_i = A_i E_i^0 \overline{\rho_i} \ln \overline{\rho_i} \quad (4)$$

Here E_i^0 is cohesive energy, which is calculated either by experiment or with DFT calculations, A_i is an adjustable parameter.

While in the original EAM method the electron density $\overline{\rho_i}$ depends only on the bond length, the Modified Embedded Atom Method (MEAM) [3, 4] includes the angular dependence of the background electron density, which describes covalent bonding more correctly [28]:

$$\overline{\rho_i} = \frac{\overline{\rho_i^0}}{\rho_0^i} \frac{2}{1 + e^{-\Gamma_i}}, \Gamma_i = \sum_{k=1}^{3} t_i^k \frac{\rho_i^{k^2}}{\rho_i^0} \quad (5)$$

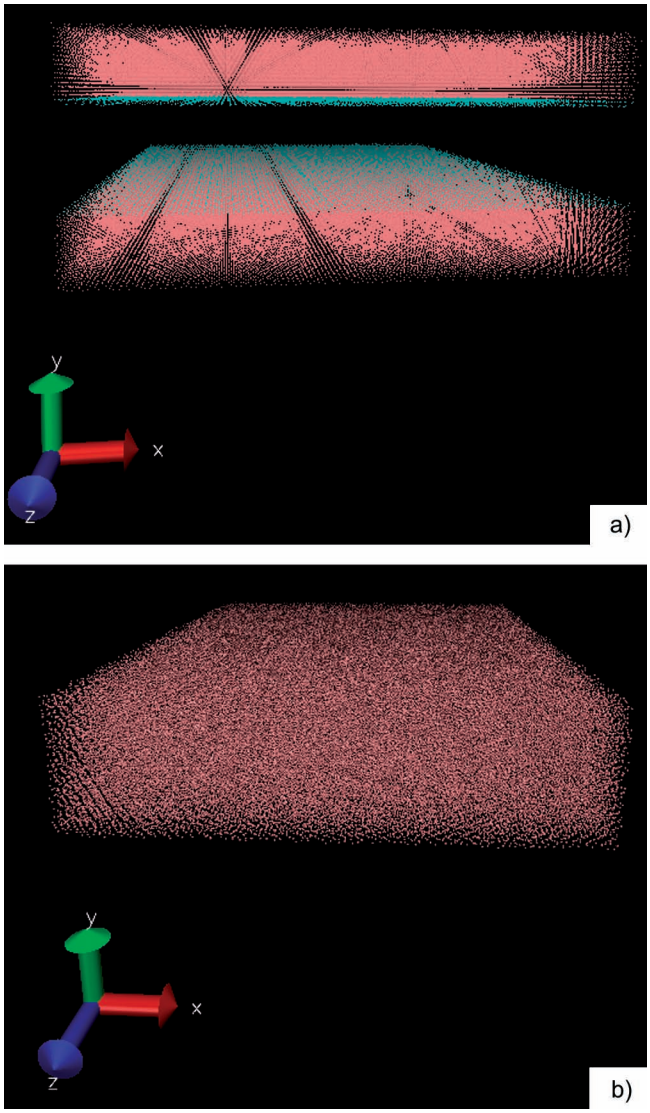

Fig. 1: Simulation boxes for surface energy calculations: (a) fractured system with two separated surfaces (marked in blue), its energy will be $E_{total}^{fracture}$; (b) bulk crystal with two surfaces combined, its energy per atom will be E_{total}^{bulk}. From these calculations surface energy is then obtained via Eq. 1.

As periodic boundary conditions were applied in this simulation, the vacuum between two separated surfaces was chosen to be 32.9 Å, which prevents the surfaces from interacting with each other.

The pair interaction potential V_{ij} from Eq. 3 depends on parameters that are calculated for reference structures (fcc Al in case of $i = j = Al$ and Al-O dimer for V_{AlO} and $i = j = O$) from Rose equation of state (see Eq. 15 in [17]). We have used the one implemented in LAMMPS software [23]. This allows the complex structure of covalent bonding to be taken into account.

The calculations were performed for hexagonal ($R3\bar{c}$) α-Al_2O_3 with lattice constants $a = b = 4.761$ Å and $c = 12.993$Å, and angles $\alpha = \beta = 90°$ and $\gamma = 120°$. The starting point of our calculations were the parameters for Al and O by Baskes [4], while the three remaining ones (cut-

off distance, attraction and repulsion parameters) were adjusted as described in [22] to reproduce melting temperature, lattice constants and elastic moduli.

The microcanonical (NVE) ensemble was used in our simulations with simulation time equal to 1000 time steps (1 ps), the temperature was kept constant during the simulation run. The resulting temperature dependence of the surface energy is shown in Fig. 2. While the interatomic potential was not tested to reproduce correct surface energies, it gives reasonable results for temperatures up to 1500 K. Above this temperature the surface energy cannot be calculated from Eq. 1 owing to slow solid-liquid phase transition.

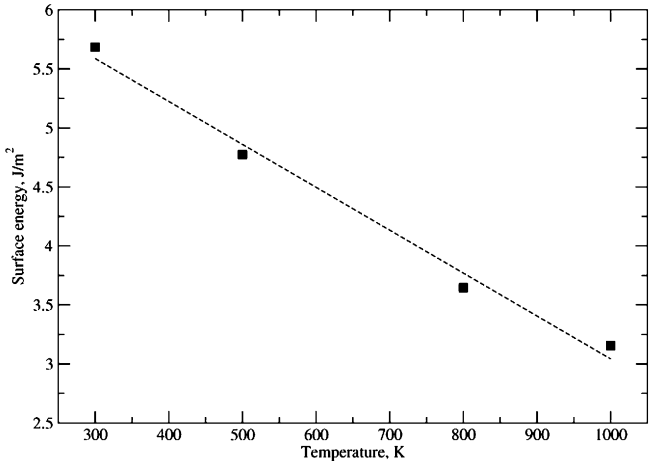

Fig. 2: Temperature dependence of the surface energy of Al_2O_3 (010) surface. Dashed line shows the linear fit.

The obtained temperature dependence of the surface energy serves as a starting point for phase field simulations of crack growth.

III. Phase Field Model

In our fracture model, which is based on linear theory of elasticity [5, 8, 26, 27], the crack has a finite tip radius $r_0 = h$, while in classical descriptions, the tip is treated as a singular point followed by a mathematical cut. The finite tip size of the crack implies that the volume inside the crack is also finite, and a description of this inner 'phase' is necessary. The crack shape in the model is not an input parameter, but it is determined self-consistently with the equations of motion. In this respect, the crack description differs significantly from classical models of fracture, where only equations of motion for the singular crack tip have to be postulated. The advantage of such a description is that the entire crack shape is a degree of freedom for the model. Therefore not only the advance of the crack itself is described, but also deformations of the crack contour behind the tip, and path selection is automatically contained.

We assume a two-dimensional plane strain situation and mode I loading, which means that the applied tensile forces act perpendicularly to the crack. On the crack contour the normal components of the stresses have to vanish, i.e. $\sigma_{nn} = \sigma_{n\tau} = 0$. These boundary conditions should be posed on the crack interface, which is not known in advance since it is the degree of freedom in our model.

The phase field method provides a powerful tool to solve such kinds of free boundary problems. The basic idea is to introduce a continuous auxiliary field Φ (phase field), which will discriminate between the different material states. We define $\Phi = 1$ for the elastic medium, and $\Phi = 0$ for the 'broken phase' with vanishing elastic moduli. Then the phase field value $\Phi = 0.5$ corresponds to the crack interface. Interpolation of the elastic constant between the two phases ensures that the boundary conditions are automatic fulfilled. It is only necessary to couple the additional phase field evolution with the force balance equation:

$$\frac{\partial \sigma_{ij}^{(el)}}{\partial x_j} = 3\alpha(3\lambda+2\mu)\frac{\partial T}{\partial x_i}, \tag{6}$$

where λ and μ are Lame constants, and α is the thermal expansion coefficient. To derive the time evolution equation for the phase field we start from a free energy functional [14]:

$$F[\phi,u_i] = \int_v (f_s + f_{d\omega} + f_{el})\, dV, \tag{7}$$

where $f_s(\nabla\phi) = 3\gamma\xi(\nabla\phi)^2/2$ is the gradient energy density and $f_{d\omega}(\phi) = 6\gamma\phi^2(1-\phi)^2/\xi$ is the double well potential, guaranteeing that the free energy functional has two local minima at $\phi = 0$ and $\phi = 1$ corresponding to the two distinct phases of the system. The form of the double well potential and the gradient energy density are chosen such that the phase field parameter ξ defines the interface width and the parameter ξ corresponds to the interface energy of the sharp interface description [11]. Finally, the elastic energy density contribution is given by

$$\begin{aligned} f_{el} &= f_0(T) - K(\phi)\,\alpha(T-T_0)\varepsilon_{ij}^2 \\ &+ \frac{K(\phi)}{2}(\varepsilon_{ii})^2 - \mu(\phi)(\varepsilon_{ij} - \frac{1}{3}\delta_{ij}\varepsilon_{kk}) \end{aligned} \tag{8}$$

where $K(\Phi)$ is a bulk modulus. The first term corresponds to the pure thermal contribution to the free energy $f_0(T) \sim T^2$. The phase field dependences of elastic moduli are given by following expressions

$$\mu(\phi) = h(\phi)\,\mu + (1 - h(\phi))\,\mu^{[b]},$$

$$K(\phi) = h(\phi)\,K + (1 - h(\phi))\,K^{[b]},$$

where μ, K and $\mu^{[b]}$, $K^{[b]}$ denote the bulk values of the moduli of the elastic medium and the 'broken phase', respectively. The function $h(\phi) = \phi^2(3 - 2\phi)$ provides an interpolation of the elastic modulu s between zero for the 'broken phase' and one for the elastic medium. It is the simplest polynomial satisfying the necessary interpolation conditions $h(0) = 0$ and $h(1) = 1$ and having a vanishing slope at $\phi = 0$ and $\phi = 1$, in order not to shift the bulk states. The elastic stresses then are defined as the derivative of the elastic free energy density with respect to the strains, i.e. $\sigma_{ik}^{(el)} = \delta f_{el}/\delta\varepsilon_{ik}$. Finally the dissipative phase field dynamics obeys the following equation

$$\frac{\partial \phi}{\partial T} = \frac{D}{3\gamma\xi}\left(\frac{\delta F}{\delta \phi}\right) \tag{9}$$

where D is the kinetic coefficient.

At this stage in order to test our approach on multiscale simulations. we performed a simulation of a temperature-driven fracture in homogeneous media. The temperature profile was fixed during the simulation and crack was propagating towards to the region of high temperature.

IV. Results and Discussion

In our previous work crack propagation under mode I loading was considered. The presence of an inhomogeneous temperature field leads to inhomogeneity of the material properties and causes the bulk forces proportional to its gradient. Typically the bulk modulus decreases with the increase of temperature, regions of the material with high temperature having a lower elastic modulus. If we apply tensile forces to such a sample with inhomogeneous distribution of temperature, the regions of lower temperature and consequently lower elastic moduli can effectively stop crack propagation. This is similar to the situation in composite materials with inclusions in the hard matrix elements with lower elastic modulus. At coherent interfaces, the elastic displacement field is continuous through the weak inclusion, therefore the elastic energy stored in the inclusion is not enough to initiate crack growth. But with the increase of temperature the surface energy also decreases. Moreover the Griffith point is inversely proportional to surface energy. Thus, the Griffith point or energy required to initiate unstable crack growth is nonlinear in dependence on temperature. And a decrease of the elastic modulus in the region of high temperature hindering crack propagation can be reversed by a decrease of surface energy, which shifts the elastic energy required for crack growth to a lower value.

To model this complicated temperature dependence, as well as to demonstrate the coupling of the phase field simulation with MD, the velocity of crack propagation under mode I loading in a constant gradient temperature field has been performed.

The temperature field does not change during the simulation and linearly increases from the left boundary of computational domain ($T = 20\ K$) to the right boundary ($T = 1400\ K$). The crack starts to growth in a region of high elastic moduli and ends in the region of lower elastic moduli. The temperature dependence of the elastic moduli has been expressed in the following form [21]:

$$\begin{aligned} E(GPa) &= 417 - 0.0525T \\ G(GPa) &= 169 - 0.0229T \end{aligned} \qquad (10)$$

while the temperature dependence of the surface energy was obtained by means of MD simulation:

$$\gamma = 3.64 - 0.00032T \qquad (11)$$

First we measure the steady state crack velocity under pure mode I loading without creation of a temperature gradient in the system, i.e. the sample has a uniform temperature $T = 20$. Next we modulate only the bulk modulus, creating a constant temperature gradient in the system. The relative decrease of the crack propagation velocity compared to the uniform temperature distribution was about 30 %. This relative crack propagation velocity reduction is proportional to the decrease of the bulk modulus. As a next step the temperature dependence of the surface energy obtained by means of MD simulation was taken into account. In this case the velocity reduction was about 2 % which is comparable to the numerical accuracy of our computation. Thus, careful calculations of the bulk modulus and especially the surface energy are required to fully capture the crack propagation features in the inhomogeneous temperate field, which is important for deriving a quantitative mechanism for crack propagation and thus improving design principles for crack-resistant ceramics as indicated above.

V. Conclusion

In conclusion, we have elucidated a scale bridging approach in its simplest form for modeling crack propagation under thermal and mechanical loading. Results of the obtained classical MD calculations, which give the temperature dependence of the surface energy, were used as input for phase field simulations at the microscale. The latter simulations were used for modeling crack propagation under mode I loading in an inhomogeneous temperature field. The temperature dependence of both the bulk moduli as well as of the surface energy plays a crucial role for the dynamics at that scale, as we could demonstrate in our simulations in the following manner: If only the temperature dependence of the bulk moduli is taken into account, the crack will encounter large deceleration of about 30 % in the high-temperature region. The addition of a surface energy temperature dependence as obtained by MD calculations changes the situation completely. The crack velocity is then still reduced, however, only by a few percent. Thus, in order to enhance our understanding of the mechanisms behind the crack propagation dynamics observed in ceramic refractories such precise multiscale models coupling physics from the nano- and microscale are required. Only these allow us to precisely predict micro crack propagation velocities for general material compositions, fillers and parameter regimes. We expect possibly yet more quantitative results from the consideration of further relevant parametric dependences from the atomic scale, which might need to be taken into account as a crucial factor at the microscale. Such advanced multi-scale approaches can thus be developed only in close comparison to advanced experimental studies, which allow access to the quality of our model developments in detail.

Acknowledgments

This work was supported by the German Research Foundation (DFG) under grant SPP 1418 Em 68/26 – 1.

References

1 Adda-Bedia, M., Arias, R., Ben Amar, M., Lund, F.: Dynamic instability of brittle fracture, *Phys. Rev. Lett.*, **82**, (11), 2314 – 2317, (1999).

2 Adda-Bedia, M., Ben Amar, M.: Stability of quasiequilibrium cracks under uniaxial loading, *Phys. Rev. Lett.*, **76**, [9], 1497 – 1500, (1996).

3 Baskes, M.: Modified embedded atom potentials for cubic materials and interfaces, *Phys. Rev. B*, **46**, 2727 – 2742, (1992).

4 Baskes, M.: Modified embedded atom method calculations of interfaces, *Sandia*, **96**, 8484, (1996).

5 Brener, E.A., Spatschek, R.: Fast crack propagation by surface diffusion, *Phys. Rev. E*, **67**, 016112, (2003).

6 Broberg, K.B.: *Cracks and Fracture*, Academic Press, (1999).

7 Daw, M., Baskes, M.I.: Embedded atom method: Derivation and application to impurities, surfaces, and other defects in metals, *Phys. Rev. B*, **29**, 6443 – 6453, (1984).

[8] Fleck, M., Pilipenko, D., Spatschek, R., Brener, E.A.: Brittle fracture in viscoelastic materials as a pattern-formation process, *Phys. Rev. E*, **83**, 046213, (2011).

[9] Freund, L.B.: *Dynamic Fracture Mechanics*, Cambridge University Press, (1998).

[10] Griffith, A.A.: *The phenomena of rupture and flow in solids*, Phil. Trans. R. Soc. Lond., 221(582 – 593):163 – 198, (1921).

[11] Gugenberger, C., Spatschek, R., Kassner, K.: Comparison of phase-field models for surface diffusion, *Phys. Rev. E,* **78**, [1], 016703, (2008).

[12] Heinz, H., Vaia, R.A., Farmer, B.L., Naik, R.R.: Accurate simulation of surfaces and interfaces of face-centered cubic metals using 12 – 6 and 9 – 6 lennard-jones potentials, *J. Chem. Phys*., **112**, 17281, (2008).

[13] Jen, S.-H., Bertrand, J.A., George, S.M.: Critical tensile and compressive strains for cracking of Al_2O_3 films grown by atomic layer deposition, *J. App. Phys*., **109**, 084305, (2011).

[14] Kassner, K., Misbah, C., Müller, J., Kappey, J., Kohlert, P.: Phase-field modeling of stress-induced instabilities, *Phys. Rev. E*, **63**, 036117, (2001).

[15] Kohn, K.: Nobel lecture: Electronic structure of matter—wave functions and density functionals, *Rev. Mod. Phys*., **71**, 1253 – 1266, (1999).

[16] Krell, A., Pippel, E., Woltersdorf, J., Burger, W.: Subcritical crack growth in Al_2O_3 with submicron grain size, *J. Eur. Ceram. Soc*., **23**, 81, (2003).

[17] Kuo, C.-L., Clancy, P.: Development of atomistic MEAM potentials for the silicon-oxygen-gold system, *Model. Simul. Mater. Sci. Eng.*, **13**, 1309 – 1329, (2005).

[18] Luan, B., Robbins, M.O.: The breakdown of continuum models for mechanical contacts, *Nature*, **435**, 929, (2005).

[19] Mehl, M.J., Papaconstantopoulos, D.A.: Applications of a tight-binding total-energy method for transition and noble metals: Elastic constants, vacancies, and surfaces of monatomic metals, *Phys. Rev. B*, **54**, 4519, (1996).

[20] Mishin, A., Farkas, D., Mehl, M.J., Papaconstantopoulos, D.A.: Interatomic potentials for monoatomic metals from experimental data and *ab initio* calculations, *Phys. Rev. B*, **59**, 3393 – 3407, (1999).

[21] Munro, R.G.: Evaluated material properties for a sintered alpha alumina, *J. Am. Ceram. Soc*., **80**, 1919 – 1928, (1997).

[22] Natanzon, Y., Pilipenko, D., Emmerich, H.: Multiscale modeling of thermoshock in aluminium oxide ceramics, *refractories WORLDFORUM*, **1**, 4, (2012).

[23] Plimpton, S.J.: Fast parallel algorithms for short-range molecular dynamics, *J. Comput. Phys.*, **117**, 1 – 19, (1995).

[24] Ramanathan, S., Fisher, D.S.: Dynamics and instabilities of planar tensile cracks in heterogeneous media, *Phys. Rev. Lett.*, **79**, [5], 877 – 880, (1997).

[25] Riko, I.M., Pramana, S.S., Rong, E.P.J., Cheong, W.C., Zhong, C., Yoong, A.T.I., Lip, G.C.: Study of metal additives to alumina substrate for high temperature and pressure application, *IEEE Electronics Packaging Technology Conference (EPTC)*, **14**, 48, (2012).

[26] Spatschek, R., Brener, E.A., Pilipenko, D.: Crack growth by surface diffusion in viscoelastic media, *Phys. Rev. Lett.*, **101**, [20], 205501, (2008).

[27] Spatschek, R., Hartmann, M., Brener, E., Müller-Krumbhaar, H, Kassner, K.: Phase field modeling of fast crack propagation, *Phys. Rev. Lett.*, **96**, 015502, (2006).

[28] Streitz, F.H., Mintmire, J.W.: Electrostatic potentials for metal-oxide surfaces and interfaces, *Phys. Rev. B*, **50**, 11996 – 12003, (1994).